JPhys Photonics

PAPER • OPEN ACCESS

Divided-pulse nonlinear compression in a multipass cell

To cite this article: Henning Stark *et al* 2022 *J. Phys. Photonics* **4** 035001

Journal of Physics: Photonics

PAPER

Divided-pulse nonlinear compression in a multipass cell

Henning Stark[1,2,*], Christian Grebing[1,2,5], Joachim Buldt[1], Arno Klenke[1,3,4] and Jens Limpert[1,2,3,4]

[1] Friedrich Schiller University Jena, Abbe Center of Photonics, Institute of Applied Physics, Albert-Einstein-Str. 15, 07745 Jena, Germany
[2] Fraunhofer Institute for Applied Optics and Precision Engineering, Albert-Einstein-Str. 7, 07745 Jena, Germany
[3] Helmholtz-Institute Jena, Fröbelstieg 3, 07743 Jena, Germany
[4] GSI Helmholtzzentrum für Schwerionenforschung, Planckstraße 1, 64291 Darmstadt, Germany
[5] Current address: Active Fiber Systems GmbH, Ernst-Ruska-Ring 17, 07745 Jena, Germany.
[*] Author to whom any correspondence should be addressed.

E-mail: lars.henning.stark@uni-jena.de

OPEN ACCESS

RECEIVED
15 February 2022

REVISED
5 April 2022

ACCEPTED FOR PUBLICATION
12 April 2022

PUBLISHED
25 May 2022

Keywords: divided-pulse nonlinear compression, multipass cells, ultrafast fiber lasers, coherent combining

Supplementary material for this article is available online

Abstract

The pulse-energy and peak-power limitations of a gas-filled multipass cell (MPC) for nonlinear pulse compression are surpassed by applying a burst of four temporally separated pulses instead of a single one. The burst is generated by two birefringent crystals and contains 1 mJ of energy per pulse replica. It is then spectrally broadened in an Argon-filled MPC and recombined into a single pulse by a second set of birefringent crystals. The combined pulse is compressed by chirped mirrors to a pulse duration of 32 fs and a pulse energy of 3.4 mJ. An excellent passive stability and a high system efficiency of >90% are reached. Using the 4-pulse burst, the overall output energy supported by the MPC is doubled in comparison to single-pulse operation.

1. Introduction

Femtosecond pulse durations and extreme pulse peak powers render ultrafast laser systems indispensable for nonlinear frequency conversion [1, 2], coherent diffractive imaging [3] and more. Typically, such applications require sub-100 fs pulses and peak powers as high as possible to start the respective process or improve its efficiency, while a high average power is desired to increase production speed or signal-to-noise ratio and reduce exposure times. The needed parameters are usually generated by a high-power amplifier scheme based on thin-disk, slab or fiber, followed by a nonlinear pulse compression stage to access the sub-100 fs regime [1, 4, 5]. While different post-compression schemes have been developed over the past decades, recently multipass cell (MPC) based approaches have gained a lot of attention [6–9]. Typically, MPCs feature a high transmission and are mostly resistant to pointing instabilities of the driving laser, allowing reliable nonlinear compression of kilowatt level average powers [5] and multi-millijoule pulse energies [4]. However, MPCs have their individual limitations, mainly posed by optical damage of the MPC mirrors and ionization of the nonlinear gas induced by the high peak intensity and fluence.

The most straightforward way of pushing the compressible laser performance is by increasing the size of the MPC and, thus, decreasing the peak intensity on the mirrors and in the gas. However, large and bulky setups are undesirable and become unfeasible at some point. Thus, new scaling techniques are developed, aiming at a reduction of the peak intensities in the MPC. This can be achieved, for instance, by altering the profile of the contained mode [10].

Alternatively, the pulse energy can be distributed in time, for instance over multiple pulse replicas. This technique was initially implemented in laser sources to increase the pulse energy extraction, where it is referred to as divided-pulse amplification [11, 12]. Later on, it was transferred to fiber-based nonlinear compression setups as divided-pulse nonlinear compression (DPNLC) [13, 14]. In this work, we report on the first successful implementation of DPNLC in an MPC compression setup [5], eventually surpassing the MPC's former limitations.

The fundamental idea underlying DPNLC is to split a single pulse into a burst of temporally separated replicas prior to nonlinear broadening, where it leads to reduced peak power and peak intensity. This, in turn, allows to postpone the onset of gas-ionization [15] and mirror damage in terms of overall input energy. Thereafter, the pulses are recombined to a single pulse exceeding the limitations of the MPC without DPNLC. Generally, such temporally recombinable bursts can be generated in different ways, either by dividing a single pulse in free-space optical delay lines [16], a set of birefringent crystals [11, 12], or by directly using a phase-manipulated pulse train from a mode-locked oscillator [17, 18]. The birefringent crystal-based approach has the major advantage of being passively stable due to its common-path design. Thus, it does not require an active interferometric stabilization to compensate environmental influences such as air fluctuations and it allows very simple, cheap and compact implementations. Consequently, the following experiment was chosen to be based on this approach.

2. Experimental setup

The pre-existing nonlinear compression setup with the DPNLC modules to be implemented is shown in figure 1. An ultrafast high-power, high-energy fiber laser system based on chirped-pulse amplification (CPA) and coherent beam combination of 16 ytterbium-doped rod-type amplifiers is used as the driving laser source [19]. The amplified and combined beam is collimated to a diameter of 8 mm and sent through a two-staged CPA compressor. Here, the first stage in ambient air removes about 90% of the pulse chirp while the second stage is placed in an aluminum chamber, which can be filled with a protective atmosphere, and finalizes the CPA compression to 175 fs in this experiment. This two-staged compressor design allows to efficiently avoid beam distortions caused by nonlinear absorption and consequential thermal load in air, which becomes a considerable limitation for longer beam propagation distances at high peak and average powers [19]. Between both compressors, the beam passes a half-wave plate (HWP) and a thin-film polarizer (TFP) for free adjustment of the finally emitted power.

The CPA-compressed output is then sent into an MPC for nonlinear spectral broadening. The MPC consists of two dielectric concave mirrors with a radius of curvature of 600 mm, facing each other in a close-to-concentric distance of 1183 mm, generating a total of 26 focal passes. The Gaussian eigenmode is calculated to have diameters of 0.30 mm in the waist and 2.5 mm on the mirrors [5]. The MPC together with the required mode-matching telescopes for the input and output beams are placed in a vacuum chamber which is typically filled with argon as the nonlinear medium at an adjustable pressure. After being coupled out of the MPC, the spectrally broadened signal is re-collimated to 8 mm diameter. The beam then leaves the MPC pressure chamber, travels about 10 cm through ambient air and directly re-enters an argon-protected environment. Here, a beam sample is taken by a broadband output coupler with 99% reflectivity and the rest of the signal is sent into a chirped-mirror compressor. In total, a dispersion of -2100 fs^2 is applied to minimize the pulse duration as measured with a following auto-correlator (AC). The corresponding signal sample is taken by a fused-silica wedge which is also used for spectral analysis.

In this configuration and with an input pulse duration of 175 fs as currently emitted by the CPA system, the MPC setup can safely support single pulse energies up to 1.8 mJ at the input side. Working beyond this value substantially increases the risk of optically induced damage of the MPC mirrors and ionization of the gas environment. To increase the pulse energy supported by this pre-existing and frequently used setup [2, 5, 20] at minimum cost, effort and space taken up, DPNLC is implemented.

The required extensions are depicted in figure 1 while a more detailed view and a mathematical description of the crystal orientations and the pulse burst generation are given in figure 2 and appendix A (available online at stacks.iop.org/JPPhoton/4/035001/mmedia), respectively. The module for pulse splitting is inserted between the CPA output and the MPC. It consists of two HWPs and two birefringent crystal plates CP1 and CP2. By CP2 having twice the thickness d of CP1, a burst of four equidistant pulse replicas is generated with a distinctive polarization pattern as represented by the red arrows in figure 2. The HWPs are oriented such that all pulse replicas contain equal pulse energies. On the one hand, this ensures the best energy distribution and, thus, minimizes intensity peaks potentially hazardous to the mirror coatings or encouraging the onset of ionization. On the other hand, it is essential that all pulse replicas accumulate similar spectral broadening and nonlinear phase in the following MPC to eventually reach the highest possible pulse recombination efficiency. While the same result could have been achieved without the two HWPs by instead simply rotating the crystal plates themselves by 45° to the input polarization, using HWPs was found to significantly simplify the experimental realization due to an increase and decoupling of the available degrees of freedom. After nonlinear spectral broadening of the newly generated burst follows the DPNLC module for recombining, consisting of two more crystal plates CP2′ and CP1′ which are identical to

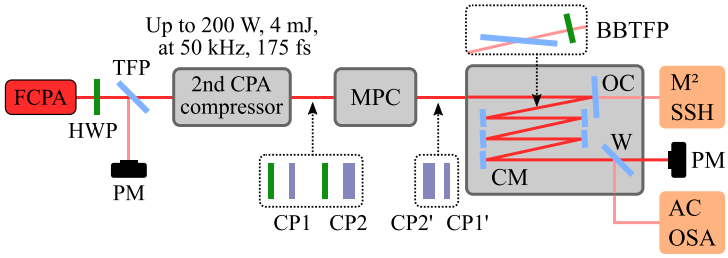

Figure 1. Schematic of the pre-existing MPC setup and the DPNLC extensions made as indicated by the dotted boxes and arrows. FCPA, fiber chirped-pulse amplification laser system [19]; HWP, half-wave plate; TFP, thin-film polarizer; CP, crystal plates; MPC, multipass cell for nonlinear broadening; CM, chirped-mirror compressor; OC, output coupler; W, wedge; BBTFP, broadband thin-film polarizer; PM, power meter; M^2, M^2-meter; SSH, spatio-spectral homogeneity analysis [5]; AC, auto-correlator; OSA, optical spectrum analyzer.

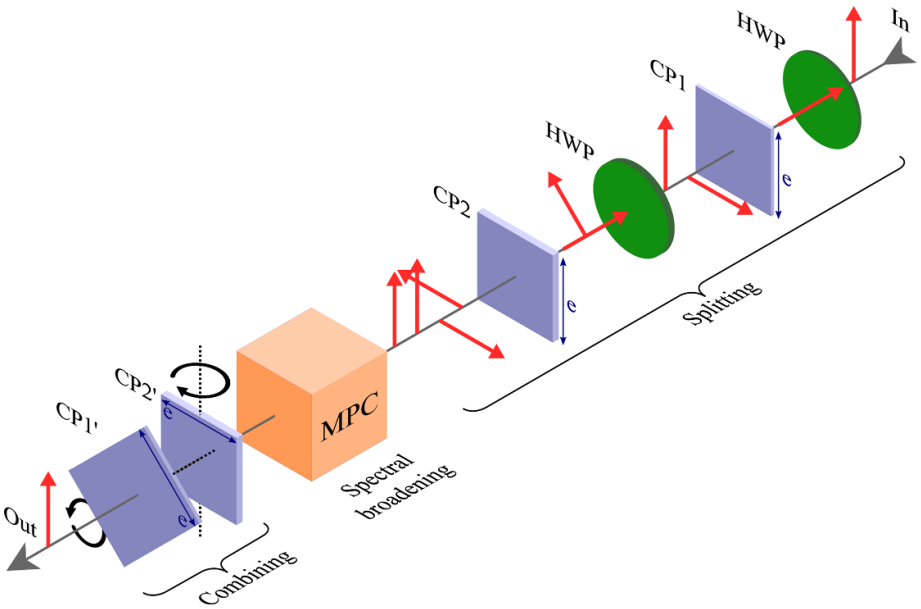

Figure 2. Implementation of birefringent crystal-based 4-pulse DPNLC to the existing spectral broadening stage. HWP, half-wave plate; CP1, CP1′, crystal plates with thickness d; CP2, CP2′, crystal plates with thickness 2 d. The extra-ordinary axes are marked with a blue arrow and labeled with an e. MPC, multipass cell for nonlinear spectral broadening.

their respective counterparts on the splitting side. The extraordinary axes of the combining crystal plates are aligned such that all pulses of the burst experience exactly the same overall optical path length counting from the beginning to the end of figure 2, i.e. all pulse replicas pass the extraordinary axis of each crystal thickness exactly once. For this, CP1′ is rotated by 45° over CP2′, finally allowing all replicas to be stacked into a single, linearly polarized pulse again.

Additionally, the mounts of CP1′ and CP2′ are equipped with a second rotation axis orthogonal to the extraordinary axis and the beam propagation direction, as indicated in figure 2. By turning the crystal plates around these axes by only a few degrees, sub-wavelength-scale delay mismatches between pulse splitting and combining caused by smallest thickness differences between C1 and C1′ or C2 and C2′ can be compensated [21]. The nonlinearly broadened and re-combined pulse passes the output coupling mirror for sampling and an additionally integrated broadband TFP, reducing residual recombination imperfections and cleaning the polarization. As before, the beam is then chirped-mirror compressed, sampled and sent onto a power meter.

For the experimental implementation, the choice of the crystal material is crucial. Besides a good high-power compatibility being inevitable, many different parameters have to be considered and weighed. A low and for both crystal axes preferably equal nonlinear refractive index reduces Kerr-lensing and combining issues. The dispersion mismatch between both crystal axes has to be as small as possible, since the spectral

bandwidths on the splitting and combining side are different. This can lead to mismatching spectral phases, hamper the combining quality and pulse contrast and, finally, become a limiting factor [13, 22, 23]. On the contrary, a strong birefringence is highly desirable, allowing thinner crystal plates for a given pulse separation, especially reducing the impact of the aforementioned considerations.

Alpha barium borate (α-BBO) meets all these requirements. Crystal thicknesses of $d = 2$ mm and $2d = 4$ mm were chosen based on the refractive indices, allowing a pulse-to-pulse separation of about 800 fs, i.e. nearly five times the pulse duration, as confirmed by AC measurements. By this, notable overlap and consequential detrimental nonlinear interaction between neighboring pulse replicas is avoided. Furthermore, broadband anti-reflective coatings reduce losses and free apertures of 25 mm by 25 mm allow placing the crystals in the collimated 8 mm-beams, rendering the nonlinear phase accumulated in the crystals negligibly small. However, at significantly higher pulse energies, larger crystal and beam diameters should be considered.

3. Results

Before actually applying DPNLC to the MPC, the expectable performance gain is estimated. Especially the limitations posed by breakdown of the MPC mirrors are crucial since exceeding the supported values results in permanent damage of the coatings. Ionization effects in the gas, in turn, are predicted to show promising scalability by DPNLC [15] and, when approaching critical values, less severe consequences such as reduced overall transmission and impaired output beam quality are expected. Thus, the correlation between the number of pulses in an incident burst and the overall energy supported by the dielectric mirror coatings are investigated in a simple test setup. For this, the MPC is blocked and a sample of the MPC mirrors is placed in front of it instead. The CPA output mostly attenuated by the HWP-TFP-combination between both CPA compressors is focused to a 150 μm-spot on the dielectric coating. The power reflected in close-to 0°-angle is measured with a power meter and tracked while the output power of the CPA is slowly increased by turning the HWP until the coating breaks down. This is done for single pulse operation, 2-pulse burst (either 2 mm or 4 mm crystal) and 4-pulse burst (both, 2 mm and 4 mm crystal). The test is repeated several times for each configuration to gain statistical reliability. As a result, using 2-pulse bursts over single-pulse operation showed an increase of the overall supported pulse energy by factor 1.6, independent of the replica separation being 800 fs or 1600 fs, i.e. if 2 mm or 4 mm crystal thickness were used. The 4-pulse burst allowed an even larger increase of factor 2.2 over single-pulse operation. Thus, presuming 1.8 mJ as the single-pulse limitation of the MPC, about 4 mJ can be expected as the maximum supported input burst energy and our target value for the 4-pulse DPNLC experiment.

The MPC is filled with 350 mbar argon as the nonlinear medium. The CPA system is set to a pulse repetition rate of 50 kHz and an average output power of 200 W, resulting in the targeted 4 mJ of energy the DPNLC-enhanced MPC compression is expected to safely support. The splitting ratios are set to generate a uniform burst by carefully adjusting the two corresponding HWPs. Then, the crystal plates C1′ and C2′ are aligned in both rotation axes for maximum combining efficiency and temporal contrast by using the side pulses in the AC trace and the ripples on the optical spectrum as quality measure. No notable heating of any crystal was observed. The resulting nonlinearly broadened, recombined, polarization-cleaned and chirped-mirror compressed signal is investigated. It has an average power of 169 W before the final sampling wedge, corresponding to an overall transmission of 84% from the CPA output. In comparison to the transmission of the nonlinear compression stage without the DPNLC extension, meaning all crystal plates, associated HWPs and the broadband TFP are removed and only a single pulse of 1 mJ is sent through the MPC, the transmission is only reduced by less than 10%. Correspondingly, the overall system efficiency of the DPNLC extension surpasses 90%.

Next, the power stability is investigated, starting with a long-term measurement over 4 h using the power meter at a sampling rate of 10 Hz. Figure 3 shows the normalized output power of both the CPA system itself (red) and the corresponding signal after DPNLC (blue). The relative standard deviation (RSD) of both traces is comparable with 0.34% (DPNLC) and 0.26% (CPA). Additionally, high-frequency noise is measured using a photodiode, allowing to evaluate the relative intensity noise (RIN) over the frequency band from 25 kHz, i.e. half the repetition rate, to 20 Hz. Similarly, DPNLC shows no noticeable negative impact here, as it led to the very same RIN of 0.5% as the CPA system itself or nonlinear compression in the MPC without DPNLC extension.

The optical spectrum is analyzed as depicted in figure 4, measuring a 20 dB-bandwidth of about 120 nm. The spectral intensity ripples correspond to residual side pulses caused by imperfect pulse recombining and, investigating the interference contrast and the Fourier transform of the spectrum, indicate that only about

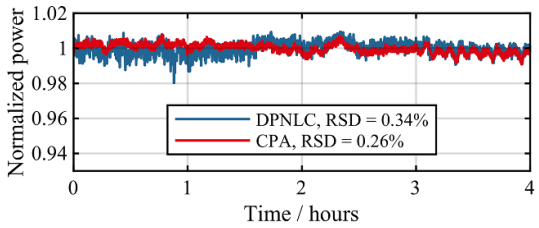

Figure 3. Normalized output power of the CPA system (red) and the compressed and recombined DPNLC signal (blue).

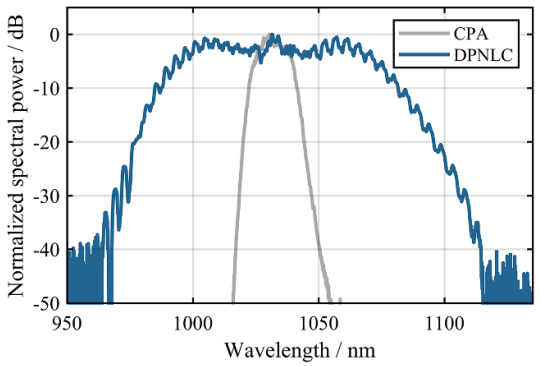

Figure 4. Spectrum of the combined and compressed signal.

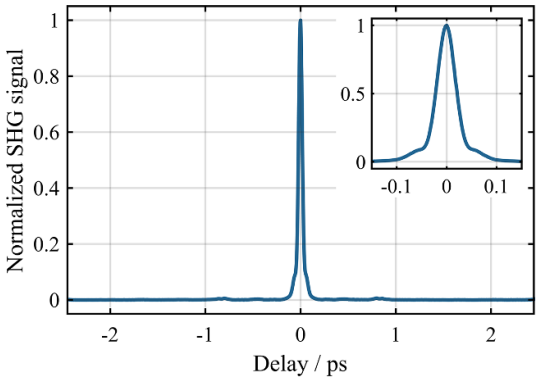

Figure 5. Auto-correlation trace of the combined and compressed signal. The inlay shows a magnification of the main pulse.

0.5% of the output energy is contained in these side features, which is negligible for most applications but has to be considered for very demanding ones. Next, the AC is investigated and its duration minimized by adding another -240 fs^2 of dispersion to compensate the crystal plates. The single clean pulse in figure 5 has a nearly transform limited pulse duration of 32 fs. Negligibly small side features can be seen in a distance of 800 fs, while none are visible at all at 1600 fs, confirming a good side-pulse contrast as estimated above and a close-to-perfect combining performance.

Additionally, the beam quality is investigated. Unfortunately, the large broadband TFP is found to introduce a slight beam deterioration presumably due to residual surface roughness and curvature. Since this is not a fundamental limitation of the DPNLC approach and it is expected to be solved by replacing this component in future, the beam quality is measured before the TFP. The result is shown in figure 6 and has the same $M^2 = 1.2$ as the laser system itself [19]. Last but not least, also the spatio-spectral homogeneity [24] is inspected with an imaging spectrograph as described in [5] and quantified to 99.3%.

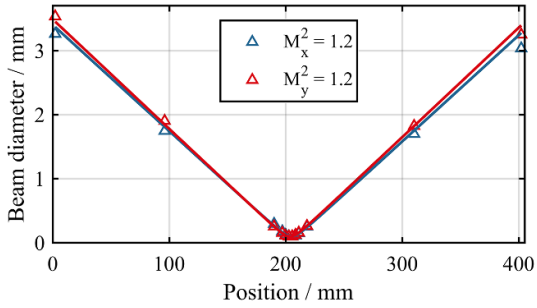

Figure 6. M^2 of the nonlinear broadened and combined signal.

4. Conclusion

In conclusion, we successfully implemented DPNLC into a multipass-cell (MPC) based nonlinear pulse compression scheme for the first time. By using bursts of four pulses for spectral broadening, the overall output pulse energy supported by the pre-existing MPC could be doubled to 3.4 mJ at an average power of 169 W. An excellent beam quality of $M^2 = 1.2$ and a spatio-spectral homogeneity of 99.3% were achieved, showing no perceivable difference to operation without DPNLC and at lower pulse energies. The technique reached a high efficiency of more than 90%, including losses due to coherent pulse recombination and additional optical elements in the beam path. The setup based on pairs of 2 mm and 4 mm thick α-BBO crystal plates is cheap, ultra-compact and completely passively stable. In addition to gas-filled MPCs as presented in this work, DPNLC is expected to allow similar scaling potential for other polarization insensitive MPC schemes as well, including those based on anti-reflective coated bulk nonlinear media [9]. Thus, DPNLC is an extremely powerful extension to easily scale the performance of pre-built MPC-based nonlinear compression stages without requiring a complete rebuilding and, when designing an MPC from scratch, it allows significant reduction of cost and size of the setup. In future, we will demonstrate the experimental applicability of this technique, extend it to more pulse replicas, thus further increasing the MPC-supported output energy, and also transfer it to a setup for few-cycle pulse compression [20].

Data availability statement

The data that support the findings of this study are available upon reasonable request from the authors.

Funding

European Research Council (835306); Fraunhofer-Gesellschaft (Cluster of Excellence 'Advanced Photon Sources'); German Federal Ministry of Education and Research (funding program Photonics Research Germany, 13N15244); Thüringer Aufbaubank (2021VF0048).

ORCID iDs

Henning Stark https://orcid.org/0000-0002-1696-8222
Joachim Buldt https://orcid.org/0000-0003-1252-0380
Arno Klenke https://orcid.org/0000-0002-6981-0808

References

[1] Kramer P L, Windeler M K R, Mecseki K, Champenois E G, Hoffmann M C and Tavella F 2020 Enabling high repetition rate nonlinear THz science with a kilowatt-class sub-100 fs laser source *Opt. Express* **28** 16951
[2] Klas R, Kirsche A, Gebhardt M, Buldt J, Stark H, Hädrich S, Rothhardt J and Limpert J 2021 Ultra-short-pulse high-average-power megahertz-repetition-rate coherent extreme-ultraviolet light source *PhotoniX* **2** 4
[3] Rothhardt J, Tadesse G K, Eschen W and Limpert J 2018 Table-top nanoscale coherent imaging with XUV light *J. Opt.* **20** 113001
[4] Kaumanns M, Pervak V, Kormin D, Leshchenko V, Kessel A, Ueffing M, Chen Y and Nubbemeyer T 2018 Multipass spectral broadening of 18 mJ pulses compressible from 1.3 ps to 41 fs *Opt. Lett.* **43** 5877
[5] Grebing C, Müller M, Buldt J, Stark H and Limpert J 2020 Kilowatt-average-power compression of millijoule pulses in a gas-filled multi-pass cell *Opt. Lett.* **45** 6250
[6] Milosevic N, Tempea G and Brabec T 2000 Optical pulse compression: bulk media versus hollow waveguides *Opt. Lett.* **25** 672
[7] Schulte J, Sartorius T, Weitenberg J, Vernaleken A and Russbueldt P 2016 Nonlinear pulse compression in a multi-pass cell *Opt. Lett.* **41** 4511

[8] Hanna M, Guichard F, Daher N, Bournet Q, Délen X and Georges P 2021 Nonlinear optics in multipass cells *Laser Photon. Rev.* **15** 2100220
[9] Viotti A-L, Seidel M, Escoto E, Rajhans S, Leemans W P, Hartl I and Heyl C M 2022 Multi-pass cells for post-compression of ultrashort laser pulses *Optica* **9** 197
[10] Kaumanns M, Kormin D, Nubbemeyer T, Pervak V and Karsch S 2021 Spectral broadening of 112 mJ, 1.3 ps pulses at 5 kHz in a LG 10 multipass cell with compressibility to 37 fs *Opt. Lett.* **46** 929
[11] Szatmari S and Simon P 1993 Interferometric multiplexing scheme for excimer amplifiers *Opt. Commun.* **98** 181–92
[12] Zhou S, Wise F W and Ouzounov D G 2007 Divided-pulse amplification of ultrashort pulses *Opt. Lett.* **32** 871–3
[13] Klenke A, Kienel M, Eidam T, Hädrich S, Limpert J and Tünnermann A 2013 Divided-pulse nonlinear compression *Opt. Lett.* **38** 4593
[14] Guichard F, Zaouter Y, Hanna M, Morin F, Hönninger C, Mottay E, Druon F and Georges P 2013 Energy scaling of a nonlinear compression setup using passive coherent combining *Opt. Lett.* **38** 4437
[15] Jenkins G W, Feng C and Bromage J 2020 Overcoming gas ionization limitations with divided-pulse nonlinear compression *Opt. Express* **28** 31943
[16] Zaouter Y, Guichard F, Daniault L, Hanna M, Morin F, Hönninger C, Mottay E, Druon F and Georges P 2013 Femtosecond fiber chirped- and divided-pulse amplification system *Opt. Lett.* **38** 106–8
[17] Stark H, Buldt J, Müller M, Klenke A, Tünnermann A and Limpert J 2019 23 mJ high-power fiber CPA system using electro-optically controlled divided-pulse amplification *Opt. Lett.* **44** 5529
[18] Zhou T, Ruppe J, Zhu C, Hu I-N, Nees J and Galvanauskas A 2015 Coherent pulse stacking amplification using low-finesse Gires-Tournois interferometers *Opt. Express* **23** 7442
[19] Stark H, Buldt J, Müller M, Klenke A and Limpert J 2021 1 kW, 10 mJ, 120 fs coherently combined fiber CPA laser system *Opt. Lett.* **46** 969
[20] Müller M, Buldt J, Stark H, Grebing C and Limpert J 2021 Multipass cell for high-power few-cycle compression *Opt. Lett.* **46** 2678
[21] Jacqmin H, Jullien A, Mercier B, Hanna M, Druon F, Papadopoulos D and Lopez-Martens R 2015 Passive coherent combining of CEP-stable few-cycle pulses from a temporally divided hollow fiber compressor *Opt. Lett.* **40** 709
[22] Guichard F, Hanna M, Zaouter Y, Papadopoulos D N, Druon F and Georges P 2014 Analysis of limitations in divided-pulse nonlinear compression and amplification *IEEE J. Sel. Top. Quantum Electron.* **20** 619–23
[23] Jacqmin H, Mercier B, Jullien A and Lopez-Martens R 2016 Manifold coherent combining of few-cycle pulses in hollow-fiber compressors *Appl. Phys.* B **122** 218
[24] Weitenberg J, Vernaleken A, Schulte J, Ozawa A, Sartorius T, Pervak V, Hoffmann H-D, Udem T, Russbüldt P and Hänsch T W 2017 Multi-pass-cell-based nonlinear pulse compression to 115 fs at 7.5 μJ pulse energy and 300 W average power *Opt. Express* **25** 20502